Clim Dyn (2011) 37:2167–2179
DOI 10.1007/s00382-010-0975-z

Seasonally asymmetric transition of the Asian monsoon in response to ice age boundary conditions

Hiroaki Ueda · Harumitsu Kuroki · Masamichi Ohba · Youichi Kamae

Received: 5 May 2010 / Accepted: 18 December 2010 / Published online: 31 December 2010

Abstract Modulation of a monsoon under glacial forcing is examined using an atmosphere–ocean coupled general circulation model (AOGCM) following the specifications established by Paleoclimate Modelling Intercomparison Project phase 2 (PMIP2) to understand the air–sea–land interaction under different climate forcing. Several sensitivity experiments are performed in response to individual changes in the continental ice sheet, orbital parameters, and sea surface temperature (SST) in the Last Glacial Maximum (LGM: 21 ka) to evaluate the driving mechanisms for the anomalous seasonal evolution of the monsoon. Comparison of the model results in the LGM with the pre-industrial (PI) simulation shows that the Arabian Sea and Bay of Bengal are characterized by enhancement of pre-monsoon convection despite a drop in the SST encompassing the globe, while the rainfall is considerably suppressed in the subsequent monsoon period. In the LGM winter relative to the PI, anomalies in the meridional temperature gradient (MTG) between the Asian continents minus the tropical oceans become positive and are consistent with the intensified pre-monsoon circulation. The enhanced MTG anomalies can be explained by a decrease in the condensation heating relevant to the suppressed tropical convection as well as positive insolation anomalies in the higher latitude, showing an opposing view to a warmer future climate. It is also evident that a latitudinal gradient in the SST across the equator plays an important role in the enhancement of pre-monsoon rainfall. As for the summer, the sensitivity experiments imply that two ice sheets over the northern hemisphere cools the air temperature over the Asian continent, which is consistent with the reduction of MTG involved in the attenuated monsoon. The surplus pre-monsoon convection causes a decrease in the SST through increased heat loss from the ocean surface; in other words, negative ocean feedback is also responsible for the subsequent weakening of summer convection.

Keywords LGM · Seasonal change · Monsoon · Air–sea–land interaction · Meridional temperature gradient

1 Introduction

The Asian monsoon is characterized by salient seasonal change, which is caused by heating contrast between the Asiatic land mass and adjacent oceans. The principal driving force for the monsoon is the latitudinal insolation gradient that is responsible for the alternation of the winter and summer monsoons (Webster 2006). In reality, however, the annual cycle of the monsoon circulation is largely distorted against the smooth seasonal insolation change through complicated air–sea–land interactions (Matsumoto 1992).

On an interannual time scale, it has been discussed for over a century that the snow-monsoon interaction over the Eurasia modulates the year-to-year changes in summer monsoon rainfall and circulation (Blanford 1884; Banzai and Shukla 1999). On the other hand, recent studies furnished evidence that the anomalous SST in the Indian Ocean relevant to the El Niño forcing could be another regulating factor for the summertime Asian monsoon intensity (e.g., Kawamura 1998; Meehl and Arblaster 2002).

As for the long-term climate change, an increase in the CO_2 concentration leads to greater warming over land than

H. Ueda (✉) · H. Kuroki · Y. Kamae
Graduate School of Life and Environmental Sciences, University of Tsukuba, Tsukuba, Ibaraki 305-8572, Japan
e-mail: hueda@kankyo.envr.tsukuba.ac.jp

M. Ohba
Environmental Science Research Laboratory, Central Research Institute of Electric Power Industry, Abiko, Japan

oceans, which will enhance the continental land–sea temperature contrast and ensuing intensified summer monsoon. However, prediction by climate models suggests that the monsoonal precipitation will increase while the circulation itself will be coincidentally weakened (e.g., Kitoh et al. 1997). The rainfall-wind paradox can be explained by large-scale heating contrast and in situ thermodynamic processes in the following manner. As for the wind fields, a decrease in the meridional thermal gradient (hereafter referred to as MTG) in the middle to upper troposphere, anchored by rainfall-related larger temperature increase over the equatorial regions, is responsible for the weakening of the monsoon circulation. In terms of the thermodynamic nature, atmospheric moisture buildup induced by the warmed oceans will result in larger moisture flux and more precipitation over South Asia (Ueda et al. 2006). In addition to the changes of the mean-field, it has been reported that the seasonal excursion of rain band will also be modulated under the increase of CO_2 concentration that may affect the duration of the rainy season (e.g., Kitoh and Uchiyama 2006). The projected changes in the late onset and withdrawal of the Baiu rainfall may be associated with the slow establishment of the Asian monsoon and related air–sea interactions (Inoue and Ueda 2009). Despite this fact, our comprehension of the fundamental controlling mechanisms remains deficient.

Given the complicated air–sea–land interaction involved in the Asian monsoon, it is natural to question whether the coupled system has changed in the past and to speculate upon near-future changes under different climate forcing. Thus, determining the sensitivity of the monsoon climate to anomalous forcing and understanding how well climate models can simulate the future state of the monsoon are critical priorities. In the framework of PMIP2, modulation of the monsoon during the mid-Holocene (6,000 years before present: 6 ka) have been focus of constant attention (e.g., Liu et al. 2003; Ohgaito and Abe-Ouchi 2007) because the air temperature was warmer than the present which bears a resemblance with projected near-future warmer climate. In the present study, we selected the Last Glacial Maximum (LGM) as an extension of our sensitivity experiments in the present (Ueda et al. 2009) and future climate (Ueda et al. 2006). The ice age is induced by the combination of seasonally different orbital forcing, anomalous ice sheet distributions, and reduced greenhouse gases that may affect the annual cycle of the Asian monsoon through changing its driving forces. Thus, studying this period will give us some insight for the monsoon dynamics. In addition, understanding how the ice age boundary condition can affect climate change is important, in particular, to examine their influence on the monsoon climate, which, in turn, has a large impact on the distribution of global precipitation. In order to cover the scarce proxy data for the precise seasonal change, we chose to examine the feedback mechanisms involved in the Asian monsoon by use of atmosphere–ocean coupled general circulation model (AOGCM) together with atmospheric GCM (AGCM) sensitivity experiments in response to different boundary conditions.

Since the pioneering research of CLIMAP project members (1976, 1981), studying this period by use of climate models as well as available geological evidence has been an important challenge confronting the climate community. The simulation at the LGM period has already been extensively conducted within the Paleoclimate Modeling Intercomparison Project (PMIP) in the last two decades. In the initial phase of PMIP (PMIP1; Joussaume et al. 1999), model-data intercomparisons were made using atmospheric general circulation models (AGCM) with prescribed CLIMAP (1981) reconstructed SST or atmosphere-mixed layer ocean models. In the second phase of PMIP (PMIP2; Harrison et al. 2002; Braconnot et al. 2007), simulations were made with coupled atmosphere–ocean GCM in which some models use dynamic vegetation model interacting with the atmosphere and ocean.

In most LGM simulations, the summer monsoon circulations weaken, and precipitation decreases (Kutzbach and Gutter 1986; Dong and Valdes 1998; Liu et al. 2007). Based on multi-model analyses, PMIP2 revealed that the former is attributed to the decreased MTG caused by the anomalous ice sheet and the latter is due to less evaporation under the cold climate. Section 2 is a description of the experimental design of the climate model. Section 3 is a presentation of the simulated seasonal evolution of the Asian monsoon, and it contains a discussion of the controlling factors by means of sensitivity experiments in response to LGM boundary conditions. Section 4 compares similarities and differences in the mechanism to modify the monsoon under different climate forcing by taking an example of future projection. Section 5 is a summary.

2 The MRI-AOGCM and boundary conditions

The AGCM is based on the global operational weather forecasting model of the Japan Meteorological Agency (JMA), which is identical to the atmospheric part of the AOGCM. Readers are referred to Shibata et al. (1999) for details. The AGCM is used for the global ocean–atmosphere coupled GCM developed at the Meteorological Research Institute (MRI; Yukimoto et al. 2006) for climate variability and change research. Here we employ a version with triangle truncation at zonal wave number 42 (T42) and 30 vertical layers on hybrid sigma-pressure coordinates. Nonlinear terms and parameterized physical processes are computed on a 128 × 64 Gaussian grid with horizontal resolution of about $2.8^\circ \times 2.8^\circ$ in longitude and latitude.

Table 1 Boundary conditions for the LGM and sensitivity experiments

Name of exp. Model type	*PI* AO-GCM	*AO-LGM* AO-GCM	*A-PI$_{CTL}$* A-GCM	*A-LGM$_{CTL}$* A-GCM	*A-LGM$_{OBT}$* A-GCM	*A-LGM$_{ICE}$* A-GCM	*A-LGM$_{SST}$* A-GCM
CO_2 [ppm]	280	185	280	185	185	185	185
CH_4 [ppb]	760	350	760	350	350	350	350
N_2O [ppb]	270	200	270	200	200	200	200
Eccentricity	0.0167724	0.018994	0.0167724	0.018994	**0.0167724**	0.018994	0.018994
Obliquity [°]	23.446	22.949	23.446	22.949	**23.446**	22.949	22.949
Precession [°]	102.04	114.42	102.04	114.42	**102.04**	114.42	114.42
Ice sheet	Present	ICE-5G	Present	ICE-5G	ICE-5G	**Present**	ICE-5G
SST	Coupled	Coupled	AO-**PI**	AO-LGM	AO-LGM	AO-LGM	**PI**

Changed conditions in A-GCM experiments are denoted in bold font

All equilibrium experiments and sensitivity experiments were performed for this study, using either present day or LGM configurations for the orbital parameters, ice sheet, and greenhouse gas concentration (Table 1). The LGM orbital parameters are identical to the PMIP protocol (eccentricity 0.018994, obliquity 22.949°, precession 114.42°). Figure 1 shows the seasonal march of the zonal-mean insolation difference between the LGM and present as a function of the latitude. The Northern Hemisphere receives more insolation in the boreal winter through the first half of spring (November $\sim$ middle of April), while it looses in summer. The phase difference between the North Pole and South Pole is about 3 months; in other words, the equatorial region gets more insolation in the boreal spring and less in the fall. The continental ice sheet reconstruction (ICE-5G ver. 1.1) is used as a boundary condition with the corresponding changes in the land–sea mask (Peltier 2004). However, vegetation remains unchanged relative to the control simulation. The greenhouse gases are lowered (CO_2 185 ppm, CH_4 350 ppb, N_2O 200 ppb) on the basis of the proxy data obtained from the ice core. The initial condition of the LGM integration is identical to the present day. Kitoh et al. (2001) also conducted the similar experiment under almost the same climate forcing. In their control experiment without fresh water preconditioning, the time series of the global mean SST gradually drop until $\sim$100 years and reaches the quasi-equilibrium state around 150 years. Hence we used the last 50 years for the analysis.

Figure 2 shows the 50-year annual mean differences of (a) surface air temperature and (b) circulation fields between LGM *minus* pre-industrial (hereafter referred to as PI). The surface air temperature falls in LGM almost all over the globe. As for the global-averaged fields, the surface air temperature is 3.2°C colder, and precipitation is 6% less (-0.15 mm day^{-1}) than PI, which is consistent with a number of LGM experiments (Braconnot et al. 2007). The largest anomaly is found over and around the Laurentide ice sheet and the Fennoscandia ice sheet due to the increase of the albedo and altitude. The largest SST drop is seen in the

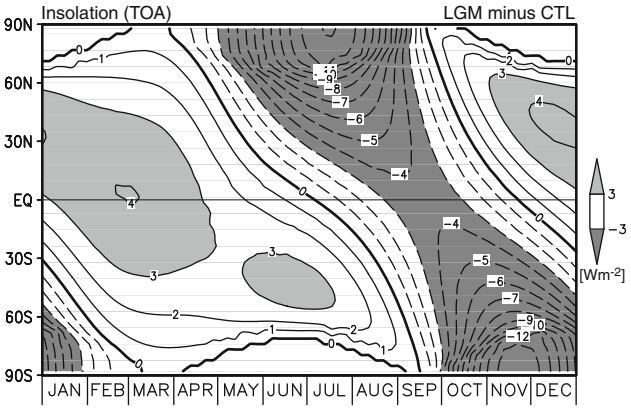

Fig. 1 Latitude-month distribution of insolation anomalies at the top of the atmosphere relative to the present day for the LGM. The contour intervals are 1.0 W m^{-2}

northwestern North Pacific and North Atlantic, which is attributed to the expansion of sea ice. Although uncertainty has been pointed about the absolute value of the reconstructed SST (e.g., Crowley 2000), the general pattern of the simulated SST in our AOGCM is fundamentally similar to the CLIMAP SST. Recently, MARGO project updated the SST reconstruction for the LGM based on 696 individual SST reconstructions in the globe except for the subtropical gyre in the Pacific Ocean (MARGO 2009), indicating pronounced cooling in the North Atlantic Ocean than those in the CLIMAP SST. In our simulation the anomalous cold SST in the North Atlantic Ocean are not recognizable, however, it is conceivable that the effect of Atlantic Ocean for the Asian monsoon is limited.

3 Results

3.1 Seasonal evolution

Figure 3a shows the longitude-time sections of precipitation and wind vectors at 850 hPa in the PI simulation along

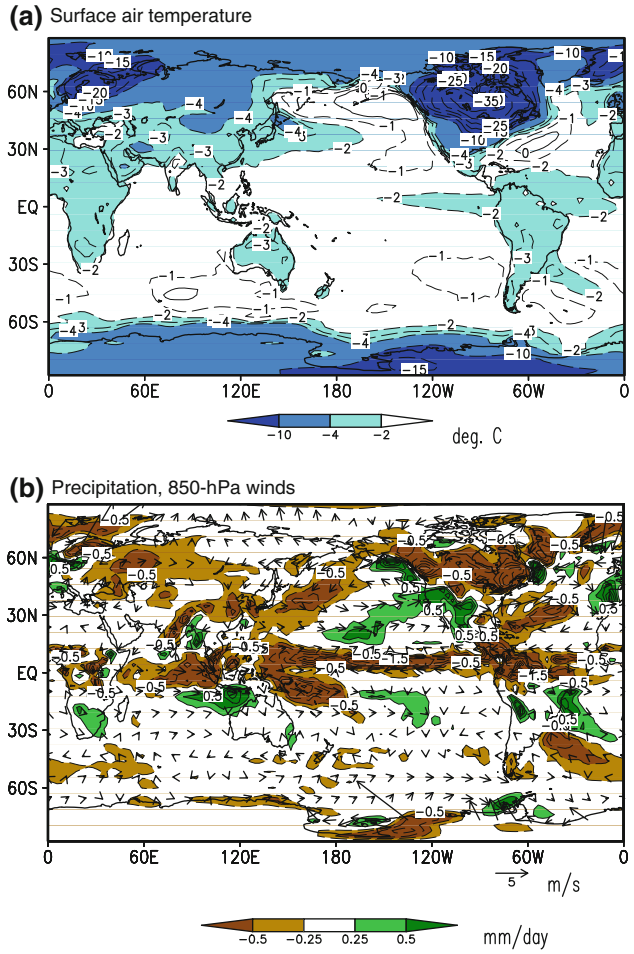

Fig. 2 Differences between the LGM and PI simulation. **a** Surface air temperature (°C), and **b** Precipitation (mm day^{-1}) with wind vectors at 850 hPa

a latitudinal band of 10°–20°N. The pre-monsoon rainfall commences first over the Indochina Peninsula (∼105°E) in April, which is consistent with the observational evidence (e.g., Matsumoto 1997). Subsequently, the planetary-scale monsoon onset, called the first transition (Lau et al. 1998), occurs in mid-May with the enhancement of rainfall and intensification of the monsoon westerlies, bearing considerable resemblance with the observations (Li and Yanai 1996; Ueda and Yasunari 1998). The summer monsoon terminates in the end of September, and succeeding seasons are characterized by the dominance of easterlies. As for the LGM anomalies in comparison with the PI simulation (Fig. 3b), anomalous precipitation over the Bay of Bengal (85°–100°E) can be seen during April and May, while the convection and low-level westerly flows over the North Indian Ocean (60°–85°E) are attenuated in the mature stage of the summer monsoon (JJAS). Thus the seasonal progress of the Asian monsoon exhibits a seasonally asymmetric nature to the onset of the Asian summer monsoon.

To see the horizontal distribution of circulation fields, we show, in Fig. 4, the LGM anomalies relative to PI during the pre-monsoon season and the mature phase of the summer monsoon. Prior to the first transition, rainfall occurs over the Indochina Peninsula and Bay of Bengal in the PI simulation, which is accompanied by weak low-level monsoon westerlies (Fig. 4a). As for the LGM anomalies (Fig. 4b), enhancement of convection takes place over the southern part of Arabian Sea and Bay of Bengal with intensification of westerlies. The opposite response is recognizable in Fig. 4d, in which the mature stage of the summer monsoon in the LGM exhibits negative anomalies in rainfall over the broad Asian monsoon regions. The notable change in summertime circulation in the PI is the enhancement of westerlies along a latitudinal band between 5°N and 15°N (Fig. 4c). On the contrary, the northward excursion of westerlies weakened in the LGM climate (Fig. 4d) but, rather remains over the equatorial Indian Ocean, which is thought to be analogous to the weaker summer monsoon in warmer climates (e.g., Kitoh et al. 1997).

The natural question that arises here is the reason for the increase of the pre-monsoon rainfall despite the negative SST anomalies. To answer it, we examine the driving forces for the Asian summer monsoon. Figure 5 shows the seasonal evolution of 200–500 hPa MTG between the Asiatic continent (20°–40°N) and the tropical Indian Ocean (0°–20°N). In the PI simulation denoted by a dashed line, the reversal of MTG occurs in mid-May and attains the maximum values in July. Subsequently, the MTG becomes negative again in September to October. These features are almost the same as those in present-day climatology (Li and Yanai 1996). As for the LGM anomalies relative to the PI (bold line), the MTG is positive except for July to August, which is consistent with the enhanced pre-monsoon circulation and weaker summer monsoon intensity. The MTG in the upper troposphere is largely affected by a combination of the release of latent heat relevant to the tropical convection and decrease in the surface temperature over higher latitudes. As for the future projection, reduction of the summertime MTG (northward negative) is attributed to the anomalous warming over the equatorial regions caused by the increase in the tropical rainfall (Ueda et al. 2006). The reverse is also true for the LGM climate that the weakened tropical rainfall is responsible for the in situ anomalous cooling, producing the positive MTG anomaly (northward positive), which is recognizable in our LGM simulation. As shown in Fig. 1, the anomalous insolation seen over the mid-latitude during the boreal fall through spring is also a pacemaker for the temperature increase over the Asiatic land mass. Conversely, the decrease of insolation in the boreal summer is concurrent with the negative MTG.

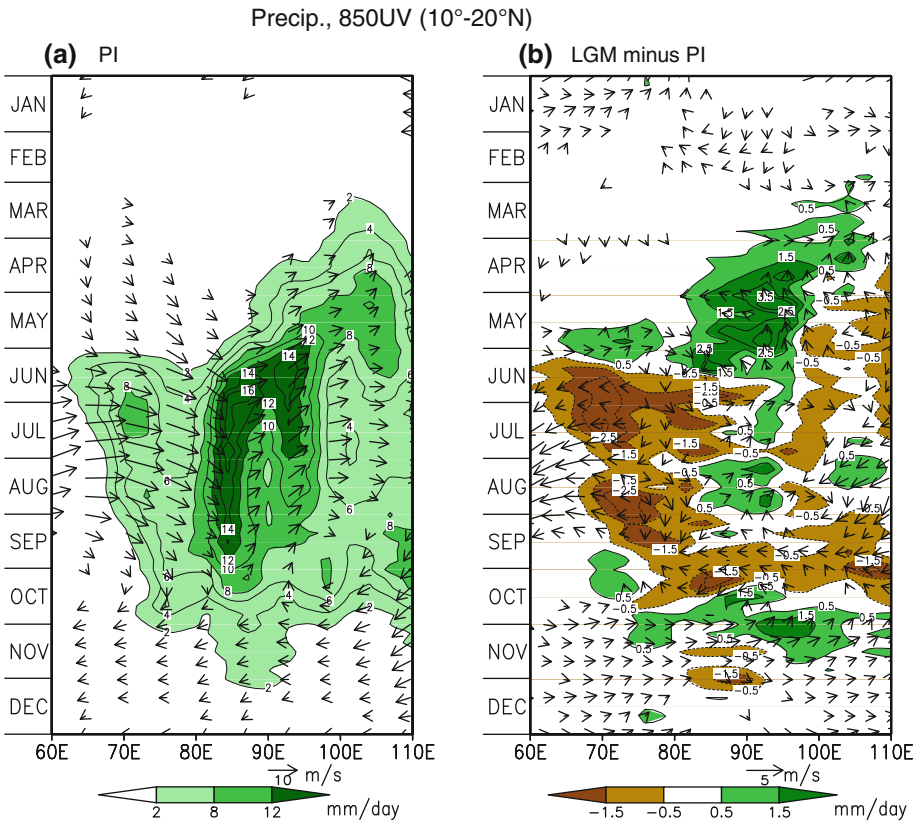

Fig. 3 Longitude-time section of pentad mean precipitation (mm day^{-1}) and 850 hPa winds averaged over 10°–20°N for **a** PI and **b** LGM minus PI

On an interannual time-scale, the meridional SST gradient in the Indian Ocean across the equators is an important player in the intensity of the Asian summer monsoon. Kawamura et al. (2003) suggested that warm/cold SST anomalies in the North/South Indian Ocean during the pre-monsoon season lead the enhancement of subsequent summer monsoon through wind-evaporation-SST feedback (Xie and Philander 1994). Annamalai et al. (2005) also showed that warm SST anomalies in the southwest Indian Ocean from March to May favor in situ enhancement of convection over the ocean, thereby delaying the onset of the Indian summer monsoon. Figure 6 shows the spatial distribution of LGM SST anomalies and also displays their seasonal evolution across the Indian Ocean. In the pre-monsoon period, negative SST anomalies are seen in the north Indian Ocean, while the rainfall increases over the Bay of Bengal and southern part of Arabian Sea (see Fig. 4b). As for the inter-hemispheric SST gradient, the SST in the Northern Hemisphere is warmer than that in the Southern Hemisphere, which is consistent with the enhanced convection. As indicated in Lindzen and Nigam (1987) using the simple one-layer model of the cumulus boundary layer, the surface pressure gradients caused by the SST gradients contribute to the low-level convergence in the tropics. Ohba and Ueda (2006) provided evidence that the value of the SST gradient of about 0.5°C/3,000 km is sufficient for the acceleration of low-level convergence through the enhancement of the low-level pressure gradient. Ueda et al. (2009) evaluated the contribution rate of the seasonal SST warming for the commencement of ASM and determined that it amounted to about 20% of the total factors, demonstrating the importance of large-scale thermal contrast. The result obtained from the present study, together with that from the other simulation (Lindzen and Nigam 1987; Ohba and Ueda 2006), suggests that the convection over the ocean, which is particularly involved in the monsoon system, could be affected by the large-scale SST distributions rather than by the in situ SST.

Wang et al. (2005) showed that, once the summer monsoon begins, the subsequent SST drops sharply due to heat loss from the ocean surface (evaporative cooling/turbulent mixing of underlying water) as well as the cloud shielding effect of solar radiation. These relationships are recognizable in our simulation. In Fig. 6b, corresponding to the mature stage of the ASM, the negative SST anomalies below −1.5°C expand northward into the southern part of the Arabian Sea and Bay of Bengal, which is attributed to the intensified heat loss from the ocean through enhanced convection in the pre-monsoon (see Fig. 4d). It is noteworthy that the latitudinal differences in the SST are not particularly large, being within the range of 0.2°C. In regard to this point, Meehl et al. (2008) have shown that enhanced pre-monsoon rainfall as a

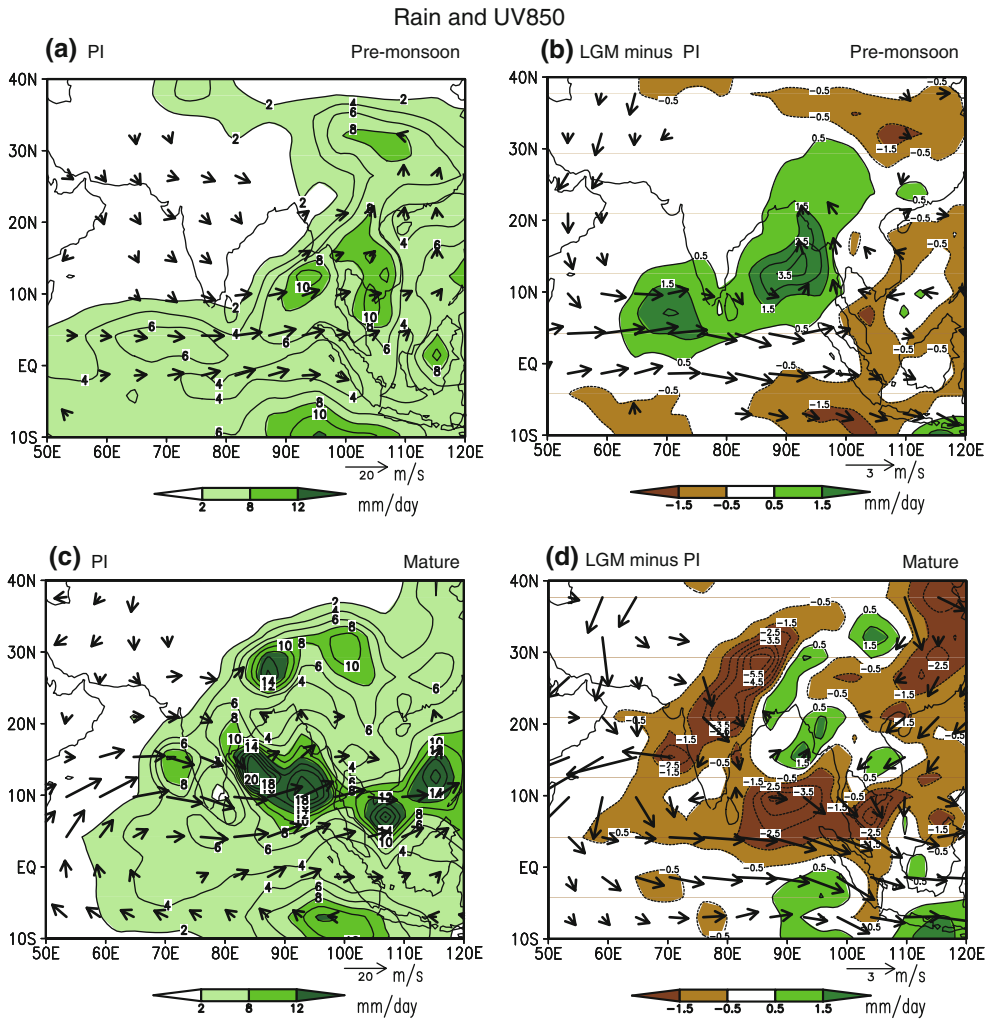

Fig. 4 LGM changes (*right panels*) in precipitation and 850 hPa winds relative to PI (*left panels*). The *upper panels* represent pre-monsoon period (April 16–May 31), the *lower panels* are mature phase (July 1–August 15). The contour interval is 2 mm day^{-1} for PI and 0.5 mm day^{-1} for the LGM anomalies. Unit vectors (m s^{-1}) are denoted in the *lower right* of each figure

consequence of black carbon aerosol induces SST decreases over the Arabian Sea and Bay of Bengal, with the largest cooling of nearly 0.15°C, contributing to the modulation of the subsequent summer monsoon. As depicted in Fig. 4c, the meridional gradient in the SST across the equator is positive from January through the first half of the summer monsoon, while the gradient becomes reversed between August and November. These results suggest that drop in the convection-induced SST is an important contributor to the seasonally asymmetric evolution of rainfall before and after the monsoon onset.

3.2 Sensitivity experiments

In this subsection, we describe the use of atmospheric GCM experiments to evaluate the contribution rate by the ocean and ice sheet feedback as well as the orbital change of the anomalous LGM climate. Three AGCM experiments were designed to quantify the individual contributions of the changes in orbital parameters, ice sheet cover, and SST for the modulation of the Asian monsoon during LGM. Note that the effect of greenhouse gas is included to the prescribed SST and ice sheet cover. Kim (2004) revealed that the reduction in atmospheric CO_2 concentration accounts for about 60% of the total LGM climate change. Table 1 shows the setup for all simulations. To compare the aforementioned parameters with the total changes, we recomputed the control values for the LGM by use of the AGCM (hereafter *A-LGM*$_{CTL}$), in which the prescribed SST is obtained from the control experiment of AOGCM in the LGM. A similar AGCM experiment was conducted for the PI (also referred to as *A-PI*$_{CTL}$). In the both control runs, we confirmed that the pattern and amplitude of precipitation in the AGCM are nearly identical to those in the AOGCM.

The effects of three boundary parameters are calculated by subtracting *A-LGM*$_{CTL}$:

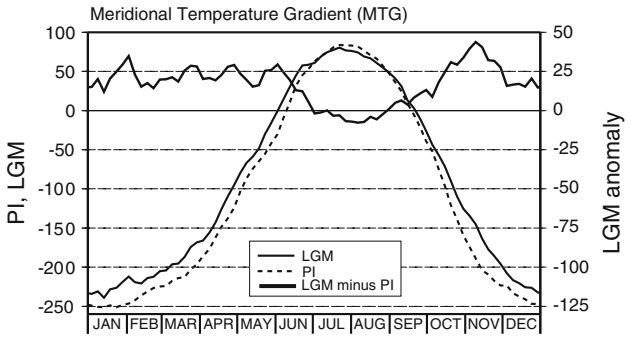

Fig. 5 Seasonal evolution of meridional difference in upper-tropospheric (200–500 hPa) thickness (m) along 70°–100°E sector between northern region (20°–40°N) minus southern region (0°–20°N). The LGM is shown with *solid line*, and the PI is given in *dashed line*. *Thick bold line* denotes LGM-PI difference (vertical scale ranges between −125 and 50 m)

$$LGM_{TOTAL} = A\text{-}LGM_{CTL} - A\text{-}PI_{CTL} \quad (1)$$

$$EFT_{OBT} = A\text{-}LGM_{CTL} - A\text{-}LGM_{OBT} \quad (2)$$

$$EFT_{ICE} = A\text{-}LGM_{CTL} - A\text{-}LGM_{ICE} \quad (3)$$

$$EFT_{SST} = A\text{-}LGM_{CTL} - A\text{-}LGM_{SST} \quad (4)$$

Here, we offer the following caveat regarding our experiments. The effects of the ice sheet cover and SST include all LGM boundary forcing because they are results of the lowered CO_2 concentration as well as the orbital information and the ice sheet. Of course non-linear interactions among various climate elements by means of positive/negative feedback are important factors for long-term amplitude modulation. Our aim is to evaluate the role of insolation difference, anomalous ice sheet distribution, and SST anomalies in the modulated seasonal evolution.

Base on Eq. 1, we compute LGM_{TOTAL} to deduce the total effect and then compare it with $A\text{-}LGM_{OBT}$, $A\text{-}LGM_{ICE}$, and $A\text{-}LGM_{SST}$ by use of the Eqs. 2, 3, and 4. Figure 7 shows the results of experiments in the pre-monsoon periods. By comparing Figs. 4b, 7a, it is confirmed that LGM_{TOTAL} is qualitatively consistent with coupled GCM experiments (*AO-LGM*), namely, enhanced rainfall over the North Indian Ocean with stronger tropical westerlies and weaker convection in the Southern Hemisphere. A comparison of LGM_{TOTAL} with EFT_{OBT}, EFT_{ICE}, and EFT_{SST} shows the contribution of boundary forcing to climate change. It is evident that the ocean feedback (Fig. 7d) to the circulation bears considerable resemblance to the LGM_{TOTAL} in spatial distribution and magnitude. The orbital change induces enhancement of precipitation over the Bay of Bengal, but its absolute values are small (Fig. 7b). No remarkable ice sheet effect over the Indian Ocean is observed (Fig. 7c).

As for the mature stage of the summer monsoon, shown in Fig. 8, the suppression of rainfall is primarily due to the

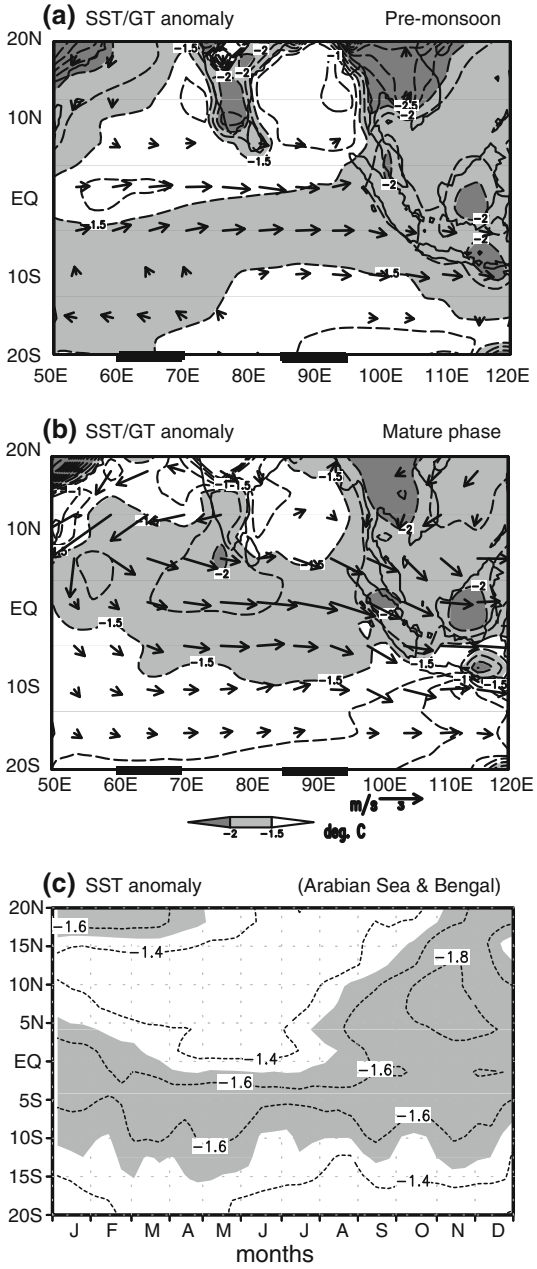

Fig. 6 LGM anomalies in the surface temperature. The horizontal distribution of SST/GT (grand temperature) for **a** the pre-monsoon period (March 1–April 15), and **b** the mature phase (July 1–August 15). The Latitude-time section of SST averaged over the Arabian Sea (60°–70°E) and Bay of Bengal (85°–95°E) is shown in the *bottom*

ocean feedback. In this stage, the prescribed SST pattern (see Fig. 6b) exhibits basin–wide cooling without a meridional SST gradient, which is consistent with attenuated convection. The other difference with the pre-monsoon period is the larger contribution of the ice sheet feedback, suggesting that the decrease in MTG (see Fig. 5) might be anchored by the decline of temperature over the Eurasian continent due to the anomalous ice sheet. Yanase

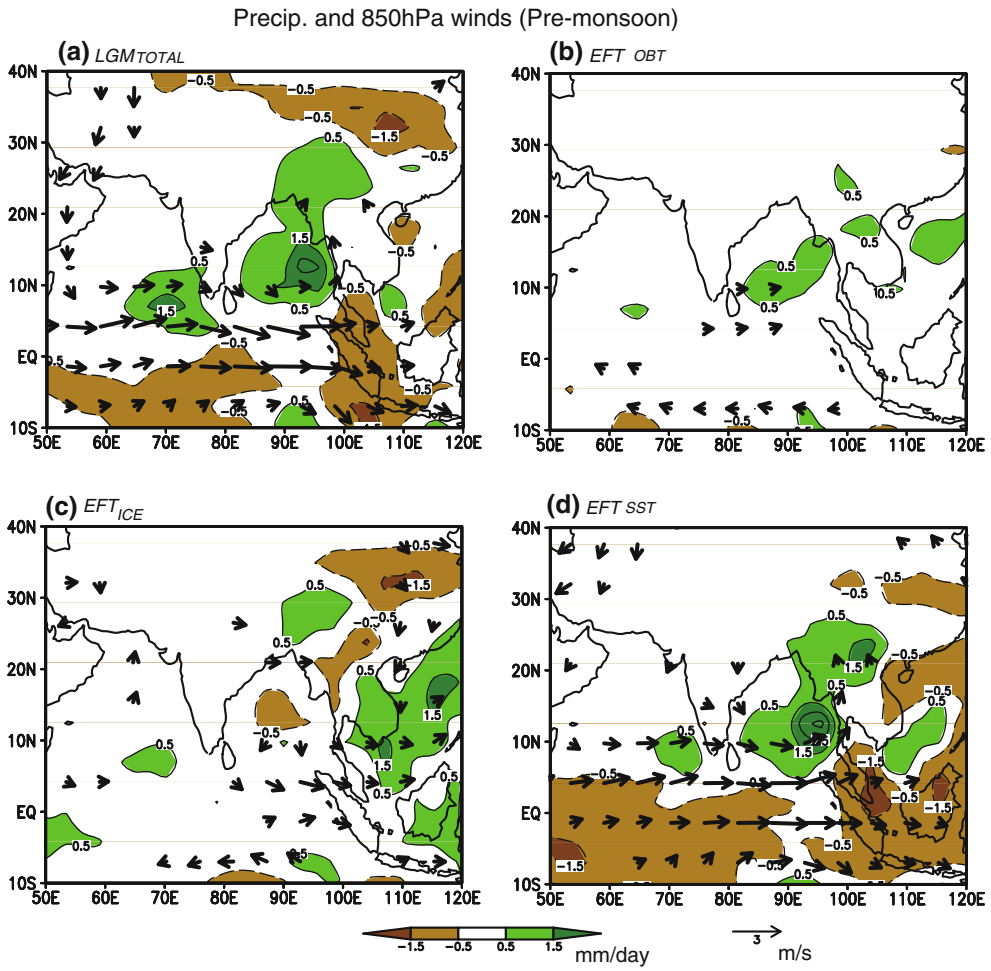

Fig. 7 AGCM sensitivity experiments for the LGM anomalies in rainfall (mm day^{-1}) and 850 hPa winds in the pre-monsoon season (April 16–May 31). **a** Control experiment of LGM by use of prescribed SST obtained from *AO-LGM*$_{CTL}$, **b** orbital effect, **c** ice sheet effect, and **d** ocean feedback

and Abe-Ouchi (2010) showed that the effect of the ice sheet is recognizable over the high-latitude North Pacific in which ice-albedo feedback in summer is larger than in winter. These differences, which are inherent in the transition of the monsoon, suggest that rainfall during the pre-monsoon season over the North Indian Ocean and adjacent regions is affected by the meridional SST gradient rather than the MTG. On the other hand, once the summer monsoon is established, its intensity is regulated by the large-scale thermal contrast in addition to ocean feedback. We also computed the residual effect by subtracting $LGM_{OBT} + LGM_{ICE} + LGM_{SST}$ from LGM_{TOTAL} (not shown). The result indicates that the spatial patterns of non-linear interaction are quite different with the total change. In other words, it is conceivable that the non-linear interaction is not dominant contributor for the total change.

Table 2 compares the effects of the orbital parameter, ice sheet distribution, and ocean feedback averaged over the Indian subcontinent and surrounding oceans, encompassing major centers of the asymmetric seasonal transition in rainfall. The SST effect dominates the pre-monsoon change, accounting for 86% of the LGM anomalies. This is consistent with the notion that the pre-monsoonal rainfall is enhanced in response to the underlying SST. The SST plays a much more important role in the summer monsoon, acting to suppress convection. When we focus on the subtropical seas, the convection-suppressing SST effect is 4 times more than the total effect of the orbital parameter and ice sheet (108% vs. −25%).

As for the mature stage over the land, the ice sheet effect is a major negative contributor for the intensity of convection, which is twice as large as the orbital effect. The reduced warming of air temperature over Asia than over the tropics, i.e., the negative MTG anomalies in the LGM, is similar to that in a warmer climate (e.g., Ueda et al. 2006); however, the fundamental controlling mechanism differs.

As mentioned before, the atmospheric temperature in the monsoon domain is mainly caused by the condensation heating, implicating an existence of the internal feedback

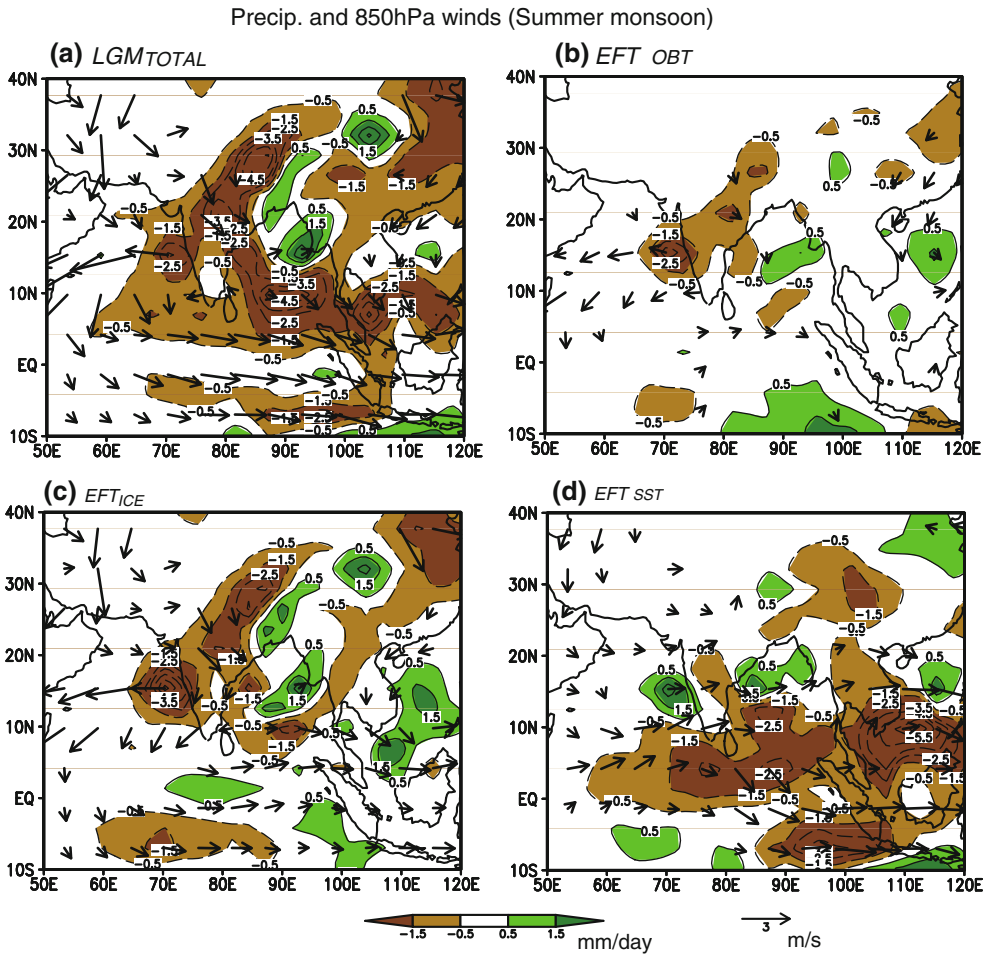

Fig. 8 Same as Fig. 7, except for the mature phase (July 1–August 15)

Table 2 Precipitation changes (mm day^{-1}) in the LGM along 70°–100°E sector, resulting from the sensitivity experiments

		LGM_{TOTAL}	EFT_{OBT}	EFT_{ICE}	EFT_{SST}
Pre-monsoon		+0.7	+0.2 (29%)	−0.1 (−14%)	+0.6 (**86%**)
Summer monsoon	Ocean	−1.2	−0.1 (−8%)	−0.2 (−17%)	−1.3 (**−108%**)
	Land	−1.0	−0.3 (−30%)	−0.6 (**−60%**)	−0.203 (−20%)

The ratio to LGM_{TOTAL} is in parentheses. The regional mean for the pre-monsoon is calculated over the subtropical region (70°–100°E, 5°–20°N). The mature stage is divided into the ocean (70°–100°E, 0–15°N) and land (70°–100°E, 20°–40°N)

Bold font denotes the values greater (less) than 50% (−50%)

between rainfall and circulation. A comparison of the atmospheric temperatures for the each experiment enable us to understand the causality between them, which will be discussed in Sect. 4.

4 Discussion

This section compares similarities and differences in the mechanism to modify the monsoon under different climate forcing by taking an example of future projection. Kitoh et al. (1997) firstly showed that the summer monsoon circulation under CO_2 doubling shifts northward toward the Asian continent. Therefore it is suggested that regionally fixed wind index in a certain area is not appropriate for climate change analysis. As for the LGM climate (see Fig. 4), the seasonal northward excursion of the summer monsoon is not found. Table 3 shows intensity change of the monsoonal wind index (Webster and Yang 1992; hereafter refereed to as WYI) for the sensitivity experiments. Prior to the summer monsoon onset, the LGM_{SST} is a dominant player for the LGM_{TOTAL}. The value of LGM_{SST} during the mature stage is

Table 3 Intensity changes of zonal wind shear (m s^{-1}) between 200 and 850 hPa over the monsoon domain (40°–110°E, 0°–20°N) during the LGM before and after the summer monsoon onset

	LGM_{TOTAL}	EFT_{OBT}	EFT_{ICE}	EFT_{SST}
Pre-monsoon	−3.0	−0.1	−0.1	−3.3
Summer monsoon	−0.2	0.6	0.5	−2.5

Values are obtained from the AGCM sensitivity experiments

also the most important contributor, while sum of LGM_{OBT}, LGM_{ICE}, and LGM_{SST} is not equivalent to LGM_{TOTAL}, implicating that the vertical wind shear index in the present climate is not suitable for the intensity change analysis.

As was mention in the Introduction, the fundamental driving force of the Asian summer monsoon is the meridional thermal gradient. Ueda et al. (2006) investigated projected future change of the Asian summer monsoon under a global warming scenario and found that the convection-induced tropical warming in the middle to upper troposphere exceeds that of the Asian continent. In other words, decrease in the meridional thermal gradient is responsible for the attenuated circulation involved in the Asian monsoon. From this perspective we investigate the LGM anomalies in the air temperature in Figs. 9 and 10. Prior to the summer monsoon onset (Fig. 9), salient cooling is found in the upper troposphere over the tropics in which the SST effect plays a dominant role. Lu et al. (2008) showed that the tropical warming in the upper troposphere under CO_2 rich atmosphere is caused by release of the latent heat associated with anomalous rainfall. The reverse

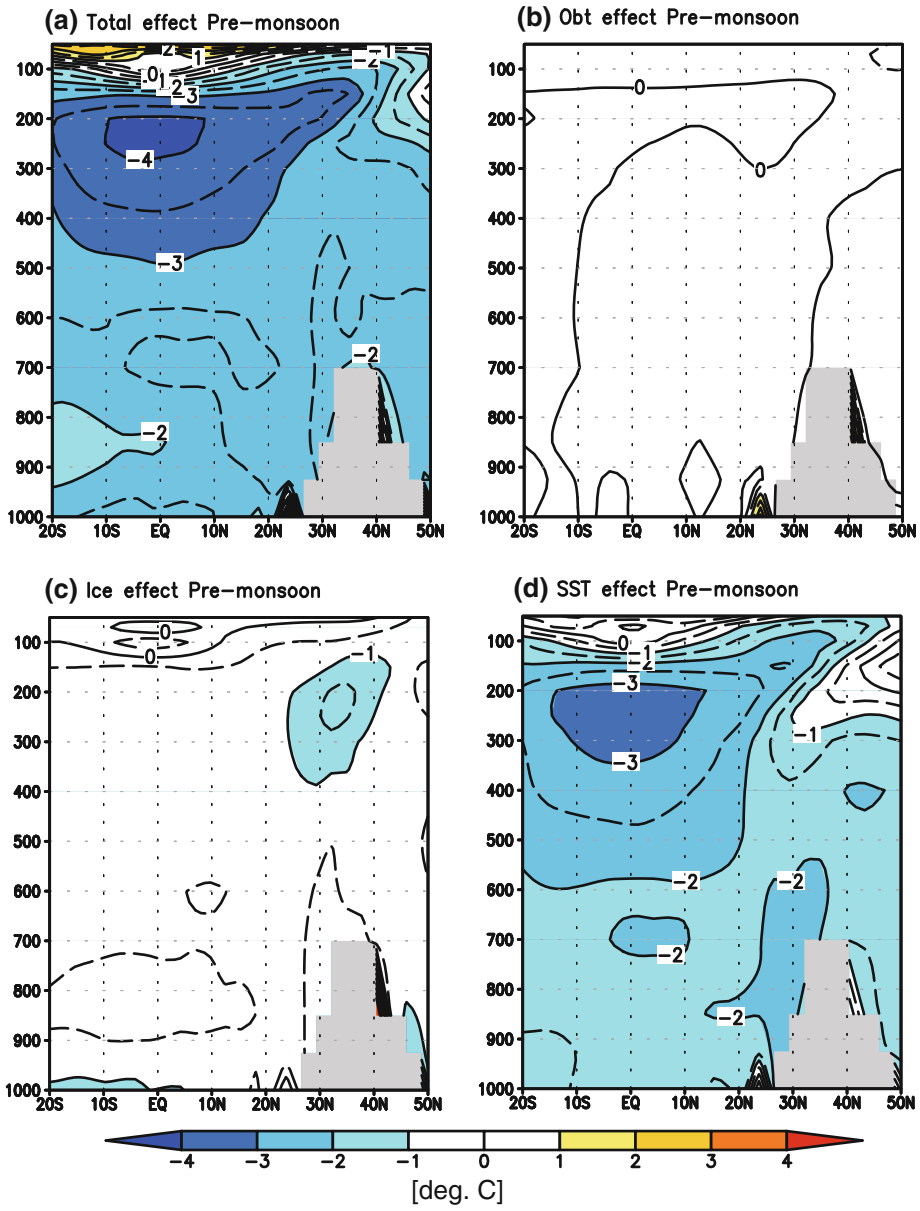

Fig. 9 Latitude-height sections of LGM anomalies in the air temperatures during the pre-monsoon season (April 16–May 31) averaged over the monsoon sector (70°–100°E). **a** Control experiment of LGM by use of prescribed SST obtained from $AO\text{-}LGM_{CTL}$, **b** orbital effect, **c** ice sheet effect, and **d** ocean feedback

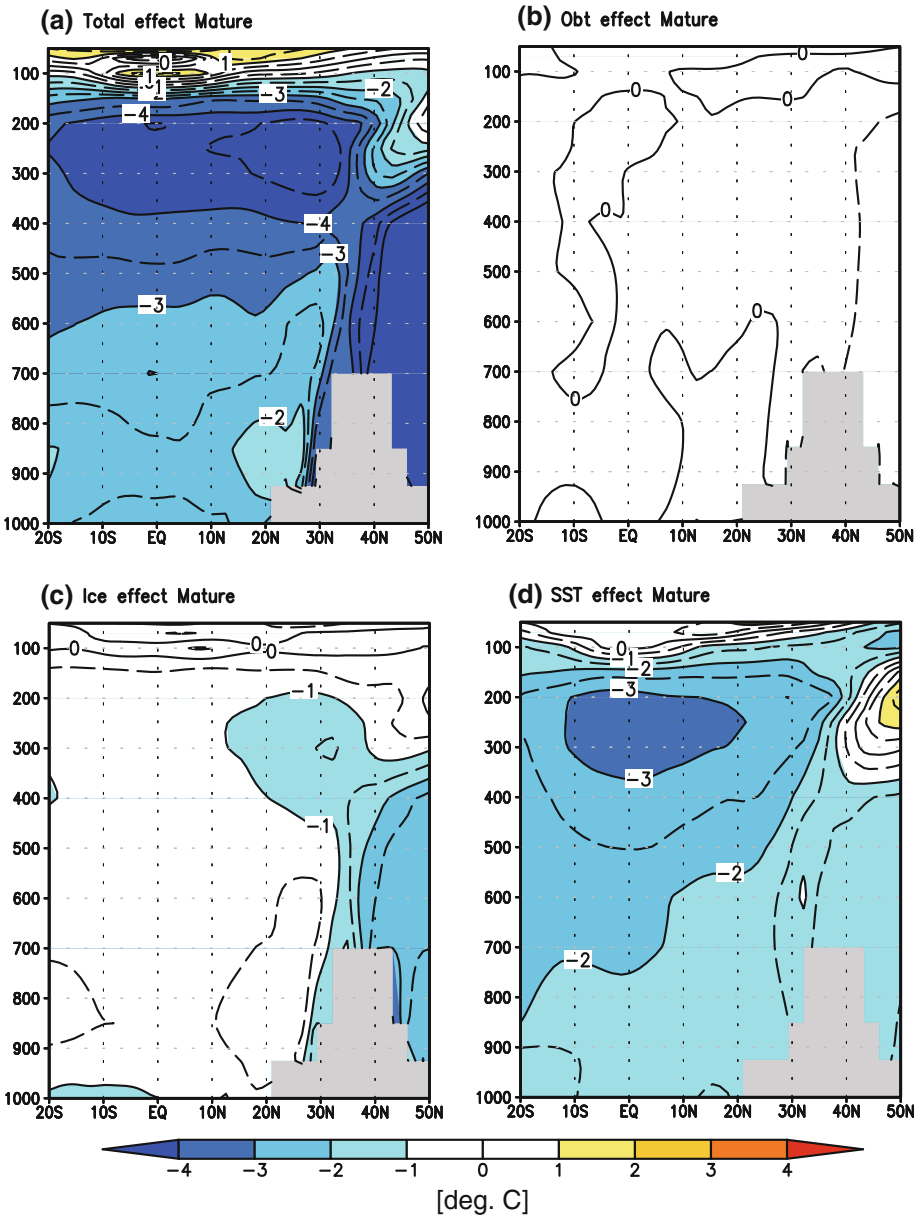

Fig. 10 Same as Fig. 9, except for the mature phase (July 1–August 15)

may be true for the LGM climate that the cold ocean could be responsible for the anomalous cooling of the upper-tropspheric air temperature through the suppressed tropical condensation heating. As for the mature period of the summer monsoon (Fig. 10), the SST effect still remains large while the ice sheet effect emerges to cool the atmospheric temperatures throughout the troposphere, which may weaken the summer monsoon circulation.

The seasonal evolution of the monsoon exhibits coupled system of atmosphere–ocean–land interaction, therefore the understanding of the inherent feedbacks is vital important issue among the monsoon community. This study shows the presence of asymmetric seasonal response to the ice age boundary forcing; an intensified pre-monsoon rainfall and subsequent weakened summer monsoon. The insolation difference could be a pace maker for these asymmetries, while the convection-induced feedback during the pre-monsoon period might be another controlling factor for the summer monsoon intensity. It is known that there are offsetting effects of convection over the North Indian Ocean for the continuing Asian monsoon intensity. Ueda et al. (2009) have shown that the decrease in the SST prior to the summer monsoon, caused by the anomalous pre-monsoon rainfall, plays a much more important role in the weakening of the succeeding summer rainfall. Their experiments were conducted under present day climatic conditions, however, the present study also suggests that the negative SST feedback prior to the summer monsoon

has a large potential for the weakening of the subsequent monsoon activity.

5 Summary

We have simulated the 21 ka climate by an ocean and atmosphere coupled model and also performed several sensitivity experiments involving glacial forcing. In terms of the annual mean (Fig. 2), the simulated 21 ka climate has common features with previous studies (Braconnot et al. 2007). In our LGM simulation, in comparison with the PI run (Figs. 3, 4), enhancement of spring rain emerges over the Bay of Bengal and Arabian Sea despite the lower surface temperature encompassing the globe, while the summertime monsoon is greatly weakened. The suppressed tropical rainfall (Fig. 2b) and resultant cooling in the upper troposphere produces the positive MTG anomaly (northward positive) that is responsible for the enhancement of the pre-monsoon circulation. The diagnosis of the LGM SST together with the sensitivity experiments in the Indian Ocean reveals that the latitudinal gradient across the equator is an additional contributor to the intensification of pre-monsoon convection (Figs. 6, 7). This suggests that the ocean monsoon could be affected by the large-scale SST distributions rather than by the in situ SST. The attenuated summertime monsoon is characterized by the inhibition of the northward excursion of monsoon westerlies toward the Asian continent, in which the continental cooling anchored by the existence of the two continental ice sheets over the northern hemisphere plays a significant role.

In summary, the results obtained from our simulation indicate that the seasonal asymmetric evolution of the monsoon in the LGM is regulated by the internal monsoon dynamics as well as the changes in boundary forcing, a finding which has potential to help us understand the maintenance and fluctuation of the monsoon in the present and future climate.

Acknowledgments This work is supported by the Global Environment Research Fund (S-5-2) of the Ministry of the Environment, Japan. The MRI makes the AOGCM available under a cooperative agreement. Comments from Dr. Tomoshige Inoue and the two anonymous reviewers helped improve the manuscript.

References

Annamalai H, Liu P, Xie S-P (2005) Southwest Indian Ocean SST variability: its local effect and remote influence on Asian monsoons. J Clim 18:4150–4167

Banzai AS, Shukla J (1999) Relation between Eurasian snow cover, snow depth, and the Indian summer monsoon: an observational study. J Clim 12:3117–3132

Blanford HF (1884) On the connexion of Himalayan snowfall and seasons of drought in India. Proc R Soc Lond 37:3–22

Braconnot P, Otto-Bliesner B, Harrison S, Joussaume S, Peterchmitt JY, Abe-Ouchi A, Crucifix M, Driesschaert E, Fichefet Th, Hewitt CD, Kageyama M, Kitoh A, Laîné A, Loutre MF, Marti O, Merkel U, Ramstein G, Valdes P, Weber SL, Yu Y, Zhao Y (2007) Results of PMIP2 coupled simulations of the mid-holocene and last glacial maximum—part1: experiments and large-scale features. Clim Past 3:261–277

CLIMAP Project Members (1976) The surface of the ice-age Earth. Science 191:1131–1137

CLIMAP Project Members (1981) Seasonal reconstructions of the Earth's surface at the last glacial maximum. Geol. Soc. Am. Map and Chart Ser., MC-36, Geol. Soc. of Am., Boulder, Colo

Crowley TJ (2000) CLIMAP SSTs re-revisited. Clim Dyn 16: 241–255

Dong B, Valdes PJ (1998) Simulations of the last glacial maximum climates using a general circulation model: prescribed versus computed sea surface temperature. Clim Dyn 14:571–591

Harrison S, Braconnot P, Hewitt C, Stouffer RJ (2002) Fourth international workshop of the palaeoclimate modelling intercomparison project (PMIP): launching PMIP2 phase II, EOS 83:447–447

Inoue T, Ueda H (2009) Evaluation for the seasonal evolution of the summer monsoon over the Asian-western Pacific sector in the WCRP CMIP3 multi-model experiments. J Meteorol Soc Jpn 87:539–560

Joussaume S, Taylor KE, Braconnot P, Mitchell JFB, Kutzbach JE, Harrison SP, Prentice IC, Broccoli AJ, Abe-Ouchi A, Bartlein PJ, Bonfils C, Dong B, Guiot J, Herterich H, Hewitt CD, Jolly D, Kim JW, Kislov A, Kitoh A, Loutre MF, Masson V, McAvaney B, McFarlane N, de Noblet N, Peltier WR, Peterschmitt JY, Pollard D, Rind D, Royer JF, Schlesinger ME, Syktus J, Thompson S, Valdes P, Vettoretti G, Webb RS, Wyputta U (1999) Monsoon changes for 6000 years ago: results of 18 simulations from the paleoclimate modelling intercomparison project (PMIP). Geophys Res Lett 26: 859–862

Kawamura R (1998) A possible mechanism of the Asian summer monsoon-ENSO coupling. J Meteorol Soc Jpn 76:1009–1027

Kawamura R, Matsuura T, Iizuka S (2003) Equatorially symmetric impact of the El NIño-Southern oscillation on the South Asian summer monsoon system. J Meteorol Soc Jpn 81:1329–1352

Kim SJ (2004) The effect of atmospheric CO_2 and ice sheet topography on LGM climate. Clim Dyn 22:639–651

Kitoh A, Uchiyama T (2006) Changes in onset and withdrawal of the East Asian summer rainy season by multi-model global warming experiments. J Meteorol Soc Jpn 84:247–258

Kitoh A, Yukimoto S, Noda A, Motoi T (1997) Simulated changes in the Asian summer monsoon at times of increased atmospheric CO_2. J Meteorol Soc Jpn 75:1019–1031

Kitoh A, Murakami S, Koide H (2001) A simulation of the last glacial maximum with a coupled atmosphere-ocean GCM. Geophys Res Lett 28:2221–2224

Kutzbach JE, Gutter PJ (1986) The influence of changing orbital parameters and surface boundary conditions on climate simulations for the past 18000 years. J Atmos Sci 43:1726–1759

Lau KM, Wu HT, Yang S (1998) Hydrologic processes associated with the first transition of the Asian summer monsoon: a pilot satellite study. Bull Am Meteorol Soc 79:1871–1882

Li C, Yanai M (1996) The onset and interannual variability of the Asian summer monsoon in relation to land-sea thermal contrast. J Clim 9:358–375

Lindzen RS, Nigam S (1987) On the role of sea surface temperature gradients in forcing low-level winds and convergence in the tropics. J Atmos Sci 44:2418–2436

Liu Z, Otto-Bliesner B, Kutzbach J, Li L, Shields C (2003) Coupled climate simulation of the evolution of global monsoons in the Holocene. J Clim 16:2472–2490

Liu X, Liu Z, Climens S, Prell W, Kutzbach J (2007) A coupled model study of glacial Asian monsoon variability and Indian ocean dipole. J Meteorol Soc Jpn 85:1–10

Lu J, Chen G, Frierson DMW (2008) Response of the zonal mean atmospheric circulation to El Niño versus global warming. J Clim 21:5835–5851

MARGO project members (2009) Constraints on the magnitude and patterns of ocean cooling at the last glacial maximum. Nat Geosci 2:127–132

Matsumoto J (1992) The seasonal changes in Asian and Australian monsoon regions. J Meteorol Soc Jpn 70:257–273

Matsumoto J (1997) Seasonal transition of summer rainy season over Indochina and adjacent monsoon region. Adv Atmos Sci 14: 231–245

Meehl GA, Arblaster JM (2002) Indian monsoon GCM sensitivity experiments testing tropospheric biennial oscillation transition conditions. J Clim 15:923–944

Meehl GA, Arblaster JM, Collins WD (2008) Effects of black carbon aerosols on the Indian monsoon. J Clim 21:2869–2882

Ohba M, Ueda H (2006) A role of zonal gradient of SST between the Indian Ocean and the western Pacific in localized convection around the Philippines. Sci Online Lett Atmos 2:176–179

Ohgaito R, Abe-Ouchi A (2007) The role of ocean thermodynamics and dynamics in Asian summer monsoon changes during the mid-Holocene. Clim Dyn 29:39–50

Peltier WR (2004) Global glacial isostasy and the surface of the ice-age Earth: the ICE-5G(VM2) model and GRACE. Annu Rev Earth Planet Sci 32:111–149

Shibata K, Yoshimura H, Ohizumi M, Hosaka M, Sugi M (1999) A simulation of troposphere, stratosphere and mesosphere with an MRI/JMA98 GCM. Pap Meteorol Geophys 50:15–53

Ueda H, Yasunari T (1998) Role of warming over the Tibetan Plateau in early onset of the summer monsoon over the Bay of Bengal and the South China Sea. J Meteorol Soc Jpn 76:1–12

Ueda H, Iwai A, Kuwako K, Hori ME (2006) Impact of anthropogenic forcing on the Asian summer monsoon as simulated by 8 GCMs. Geophys Res Lett 33:L06703

Ueda H, Ohba M, Xie SP (2009) Important factors for the development of the Asian-Northwest Pacific summer monsoon. J Clim 22:649–669

Wang B, Ding Q, Fu X, Kang IS, Jin K, Shukla J, Doblas-Reyes F (2005) Fundamental challenge in simulation and prediction of summer monsoon rainfall. Geophys Res Lett 32:L15711

Webster PJ (2006) The development of a holistic view of the monsoon. In: Wang B (ed) The Asian monsoon. Springer/Praxis Publishing Co., New York, p 787

Webster PJ, Yang S (1992) Monsoon and ENSO: selectively interactive systems. Q J Royal Meteorol Soc 118:877–926

Xie SP, Philander SGH (1994) A coupled ocean-atmosphere model of relevance to the ITCZ in the eastern Pacific. Tellus 46A:340–350

Yanase W, Abe-Ouchi A (2010) A numerical study on the atmospheric circulation over the midlatitude North Pacific during the last glacial maximum. J Clim 23:135–151

Yukimoto S, Noda A, Kitoh A, Hosaka M, Yoshimura H, Uchiyama T, Shibata K, Arakawa O, Kusunoki S (2006) Present-day and climate sensitivity in the Meteorological Research Institute coupled GCM version 2.3 (MRI-CGCM2.3). J Meteorol Soc Jpn 84:333–363